

CONSIDERATIONS FOR OPTIMIZING THE FLIGHT PERFORMANCE OF miniUAVs

Vasile PRISACARIU

”Henri Coandă” Air Force Academy, Braşov, Romania (prisacariu.vasile@afahc.ro)

DOI: 10.19062/2247-3173.2023.24.24

Abstract: Unmanned aerial vehicles benefit from a series of mature technologies that transform them into data acquisition, processing and dissemination tools with high levels of impact on areas of interest and great utility for users.

The paper exposes the stages of analysis regarding the upgrade process of UAV (ATM-1) from the variant of equipping a target aircraft to a superior variant that can be used for data collection, from areas of interest, in the form of static or dynamic images. The proposed variant has implications both on the air vector balance and on the performance of use due to the new onboard equipment.













Keywords: ATM-1, aerodynamic performances, autopilot, XFLR5 freeware

Symbols and acronyms

AGL	Above Ground level	LLT	Lifting line theory
AoA	Angle of Attack	LOS	Line of Sight
BEC	Battery Eliminator Circuit	MAC	Main Aerodynamic Chord
BLOS	Beyond Line of Sight	PDB	Power Distribution Board
C_b, C_d, C_m	Aerodynamic coefficient	Rx / Tx	Receiver / Transmitter
C2	Command and control	VLM	Vortex Lattice Method
ESC	Electronic Speed Control	XFLR5	Xfoil low Reynolds
FPV	First Person View		

1. INTRODUCTION

The paper focuses on the aerodynamic aspects of the upgrade process applied to an aircraft by exposing the stages of analysis applied to an UAV (ATM-1) from the variant of equipping a target aircraft to a superior variant that can be used for sampling data from areas of interest, in the form of static or dynamic images. The proposed aerodynamic variant has implications both on the balance of the air vector and on the performance of use due to the new onboard equipment.

Micro				Mini				Close Range				Short Range			
															
Aerovironment, USA				SkyLark, Israel				Silverfox, USA				Sojka, Czech Rep.			
Medium Range				Medium Range Endurance				Low Altitude Deep Penetration				Low Altitude Long Endurance			
															
Shadow 200, USA				Wachkeeper, Israel				CL 289, France-Germany				Eagle Scan, USA			
Medium Altitude Long Endurance				High Altitude Long Endurance				Unmanned Combat Aircraft				Optionally piloted, convertor UAS			
															
Predator A, USA				Global Hawk, USA				Barakuda, Germany				Heti ID, UK			

a
b

NATO UAS CLASSIFICATION						
Class	Category	Normal Employment	Normal Operating Altitude	Normal Mission Radius	Primary Supported Commander	Example Platform
Class II (> 600 kg)	Strike/Combat**	Strategic/National	Up to 65,000 ft	Unlimited (BLOS)	Theatre	Reaper
	MALE	Strategic/National	Up to 65,000 ft	Unlimited (BLOS)	Theatre	Global Hawk
	MALE	Operational/Theatre	Up to 45,000 ft MSL	Unlimited (BLOS)	JTF	Heron
Class I (150 kg-600 kg)	Tactical	Tactical Formation	Up to 18,000 ft AGL	200 km (LOS)	Brigade	Hermes 450
Class I (< 150 kg)	Small (<15 kg)	Tactical Unit	Up to 5,000 ft AGL	50 km (LOS)	Battalion, Regiment	Scan Eagle
	Mini (<15 kg)	Tactical Sub-unit (manual or hand launch)	Up to 3,000 ft AGL	Up to 25 km (LOS)	Company, Platoon, Squad	SkyLark
	Micro** (<66 J)	Tactical Sub-unit (manual or hand launch)	Up to 200 ft AGL	Up to 5 km (LOS)	Platoon, Squad	Black Widow

FIG. 1 UAV classification, a. civilian classification, b. NATO classification [1]

A series of specialized paper [1, 11, 12] offer classifications according to relevant criteria such as: total mass, flight duration/distance or from the point of view of use, the most relevant classifications are shown in Fig. 1.

The study stages include aspects of: description of the miniUAV variants (ATM-1 and ATM-1AP /autopilot); the XFLR5 freeware tool; comparative 2D (airfoil) and 3D aerodynamic analyzes of proposed aerodynamic concepts.

2. RESOURCES

2.1. Target drone performances.

The ATM-1 target aircraft (see Fig. 2) is based on a simple monoplane aerodynamic concept with a mid-wing, classic wing and fixed wing landing gear. Its construction is modular for both easy containerized transport and minimal time for operation in the areas of interest (pre-assembled fuselage and engine with tail-planes and landing gear, two half-planes).

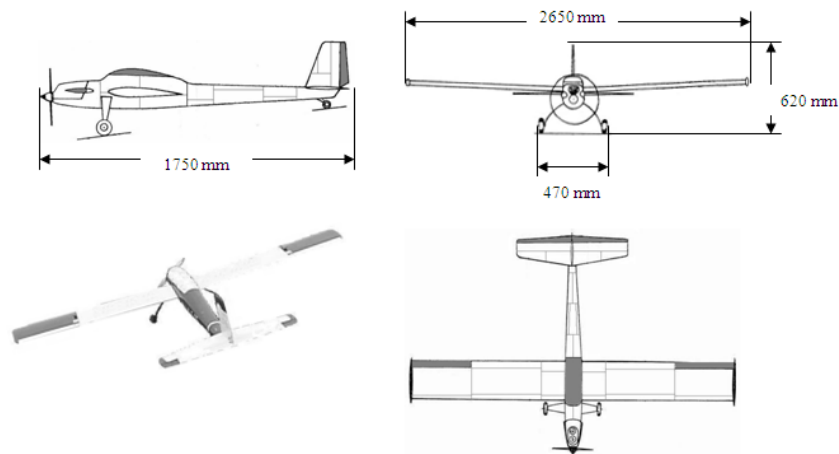


FIG. 2 Target ATM -1 [2]

The main characteristics and flight performance, in the basic version, are highlighted in Table 1.

Table 1 ATM-1 features [2, 8]

Features	Value	Features	Value
Span / Length	2650 mm / 1750 mm	Flight autonomy	0,6 h
Chord	300 mm	Flight distance	2800 m
Wing area	0,78 m ²	Ceiling	2800 m
Total weight	8 kg	Engine	26 cm ³ / 1,7 CP

2.2. ATM 1N target drone. Upgrade proposal.

For an upgrade process with a relevant performance increase, we propose a series of equipment (propulsion and radio electronics) that generate the values of new constructive characteristics highlighted in Table 2, [3, 4, 5, 8, and 9].

Table 2 Equipment and features proposal for ATM-1AP

Features	Value	Features	Value
Span / Length	2650 mm / 1750 mm	Autopilot	Pixhawk PX4
Wing area	0,78 m ²	Meteo sensor	uRad monitor A3
Total weight / payload	7 kg / 4kg	C2 system	FR Sky Taranis
Combustion engine	26 cm ³ / 2,95 CP	FPV camera	Fixed / mobile

Upgrade equipment has minimal aerodynamic implications due to forward resistance but involves centering optimizations depending on the flight range (fuel reserve). Figure 2 provides a global view of the connections and system elements on board the ATM-1AP/autopilot UAV.

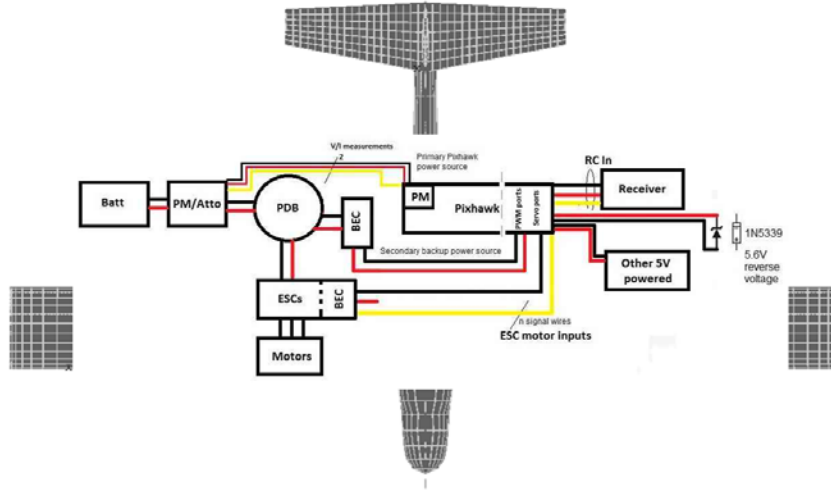


FIG.2 ATM-1AP connection diagram, [7]

2.3. Method and tools analysis

To support the upgrade process, we used the XFLR5 freeware tool that offers geometric parameterization and aerodynamic analysis modules, the latest version containing numerical calculation modules, the most relevant being: 2D design and analysis mode (aerodynamic profiles) and 3D design and analysis mode (wing, aircraft). It should be noted that these numerical analyzes are specific to the speeds and no. Low Reynolds based on LLT (lifting line theory), VLM (vortex lattice method) and 3D panel calculation methods. [6, 8].

3. PERFORMANCES ANALYSIS

3.1. Purpose, objectives and conditions of analysis

The purpose of the numerical multicriteria analysis focuses on determining the implications of the upgrade process on the overall performance of the UAV. The pursued objectives want the quantification of the analyzed parameters according to the selected analysis conditions. The analysis matrix provides a series of relevant cases for this type of miniUAV, according to Table 3.

Table 3 The analysis matrix

UAV type	2D Analysis	3D Analysis	Mass and balancing
ATM-1	yes	yes	no
ATM-1AP	yes	yes	yes

3.2. 2D and 3D aerodynamic analyzes

a. 2D analyzes

The 2D aerodynamic analyzes are focused on the numerical simulations of the profiles used in the compared construction variants, see fig. 3, under the conditions selected from table 4.

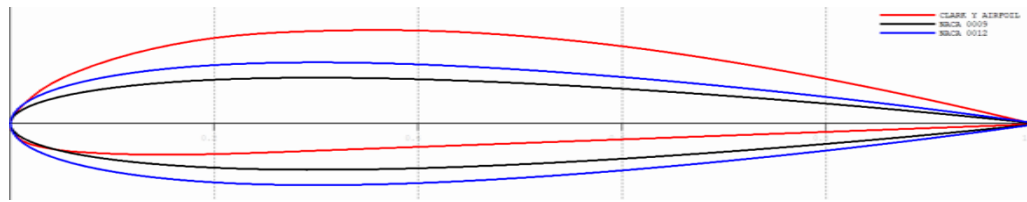


FIG. 3 The airfoils [10]

The relevant aerodynamic parameters in Fig. 4-7 (and Appendix 1) were determined by considering the viscosity effect and according to the analysis conditions in Table 4.

Table 4 The 2D analysis conditions

Condition	Value	Condition	Value
Speed	20 m/s	Iteration	100
Nr. Reynolds	400000	AoA	-15° to 15°

Figure 4 shows the variation of the lift coefficient (C_l) as a function of the angle of attack (AoA) for the analyzed profiles, due to the curvature the Clark Y profile has the highest C_l value for a fixed AoA (ex. 10°) but also a forward resistance (C_d) at the same AoA (ex.10°), see figure 5.

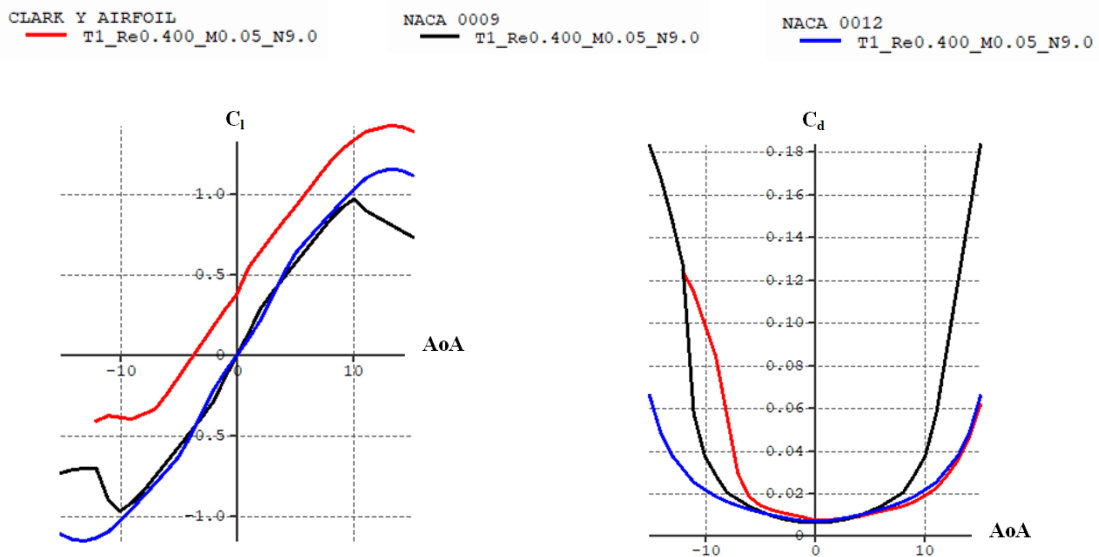


FIG. 4 C_l vs AoA

FIG. 5 C_d vs AoA

According to figure 6 we observe similar values of C_m for the symmetric profiles NACA 0009 and NACA 0012 and high values of C_m for Clark Y, values read in the range $AoA = -10^\circ \div 10^\circ$. Figure 7 shows the variation of C_l/C_d ratio vs AoA (gliding ratio) or gliding rate with high values for the Clark Y profile.

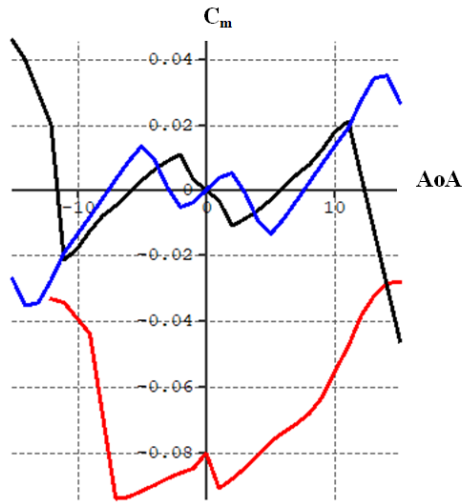


FIG. 6 C_m vs AoA

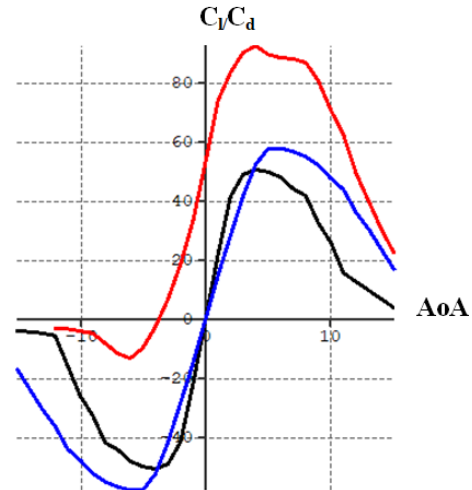


FIG. 7 C_l/C_d vs AoA

b. 3D analyzes

The values of the global geometry are similar to the ATM-1 variant, (see figure 8), the geometric configuration that was used for the initial numerical simulations, with the FPV camera nacelle mounted on the ventral side on the vertical axis passing through the leading edge of the wing. The 3D analysis conditions are recorded in Table 5.

Table 5 The 2D analysis conditions

Conditions	Value	Conditions	Value
Polar type	Fixed speed	Iterations	100
Speed	20 m/s	AoA	-15° to 15°
Type analysis	VLM	Nr. Reynolds	400000
Boundary conditions	Dirichlet		

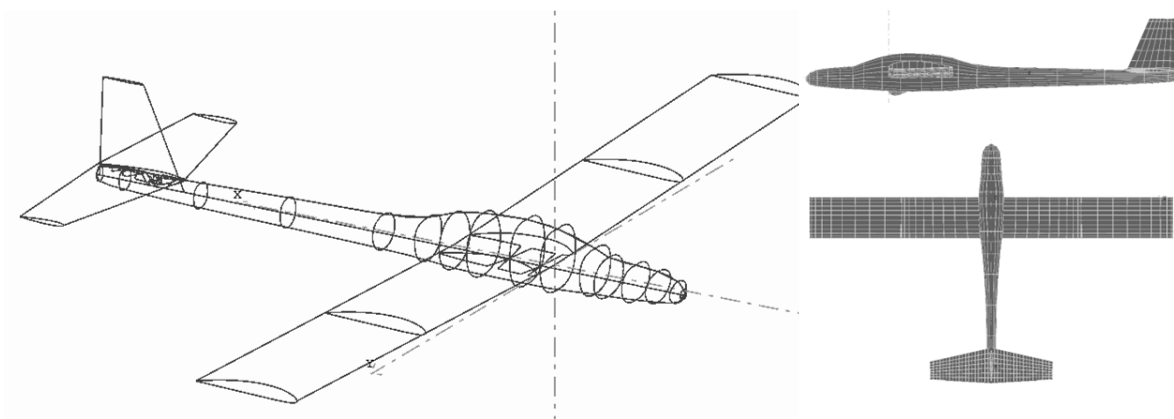


FIG. 8 ATM-1AP upgrade

In the graphs in Fig. 9-12, a series of variations of the numerical values of the aerodynamic coefficients can be observed depending on the angle of attack (AoA). In Fig.9, as expected, implications on the increase in forward resistance (C_d -AoA) and according to Fig. 10 implications on the pitching moment (C_m -AoA) are revealed.

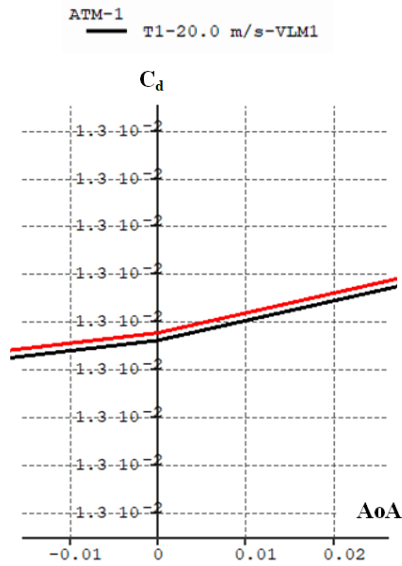


FIG. 9 C_d vs AoA

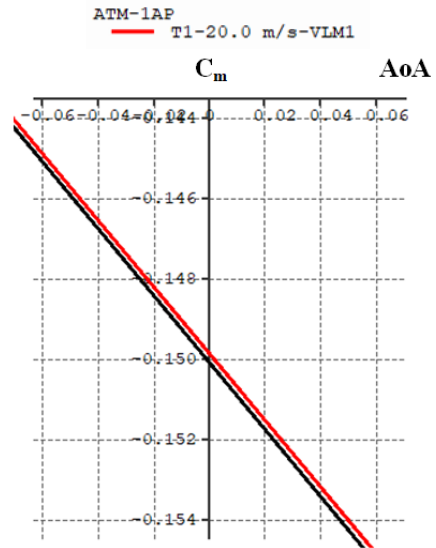


FIG. 10 C_m vs AoA

The presence of the FPV nacelle indicates a minimal influence for the roll coefficient (Fig. 11) and the yaw moment variation is maximum around the value $AoA=10^\circ$ (Fig. 12).

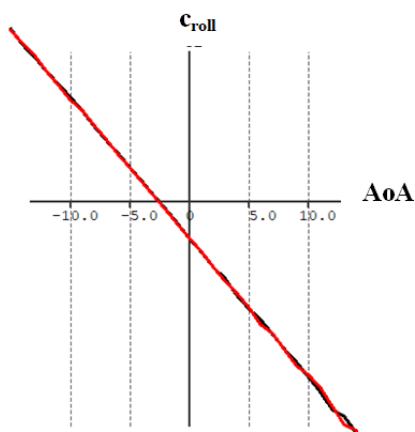


FIG. 11 C_{roll} vs AoA

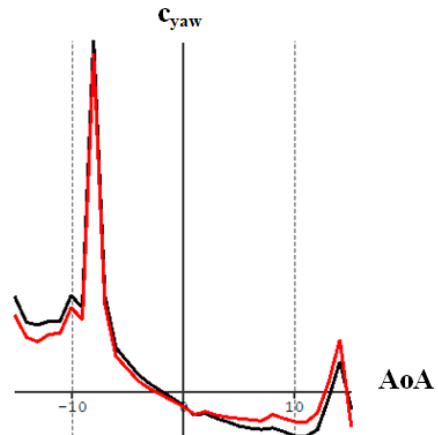


FIG. 12 C_{yaw} vs AoA

c. Balancing

The mass estimate for the onboard equipment is highlighted in Table 6.

Table 6 The mass estimate (kg)

Nr. crt.	Elements	ATM-1	ATM-1AP
1	Wing	2,2	2,2
2	Fuselage	2,3	2,3
3	Horizontal tail	0,3	0,3
4	Vertical tail	0,2	0,2
5	Engine	1,7	1
6	FPV camera	0	0,05
7	Autopilot + receiver	0,3	0,1
8	Fuel	1	1
9	Battery	0	0,25
	Total	8,0	7,40

The arrangement of the masses on the air vector can be seen in figure 11, and the numerical data in annex 3. When arranging the masses of the equipment, both the availability of the volumes of the front fuselage (for the tank) and of the rear fuselage for the autopilot were taken into account.

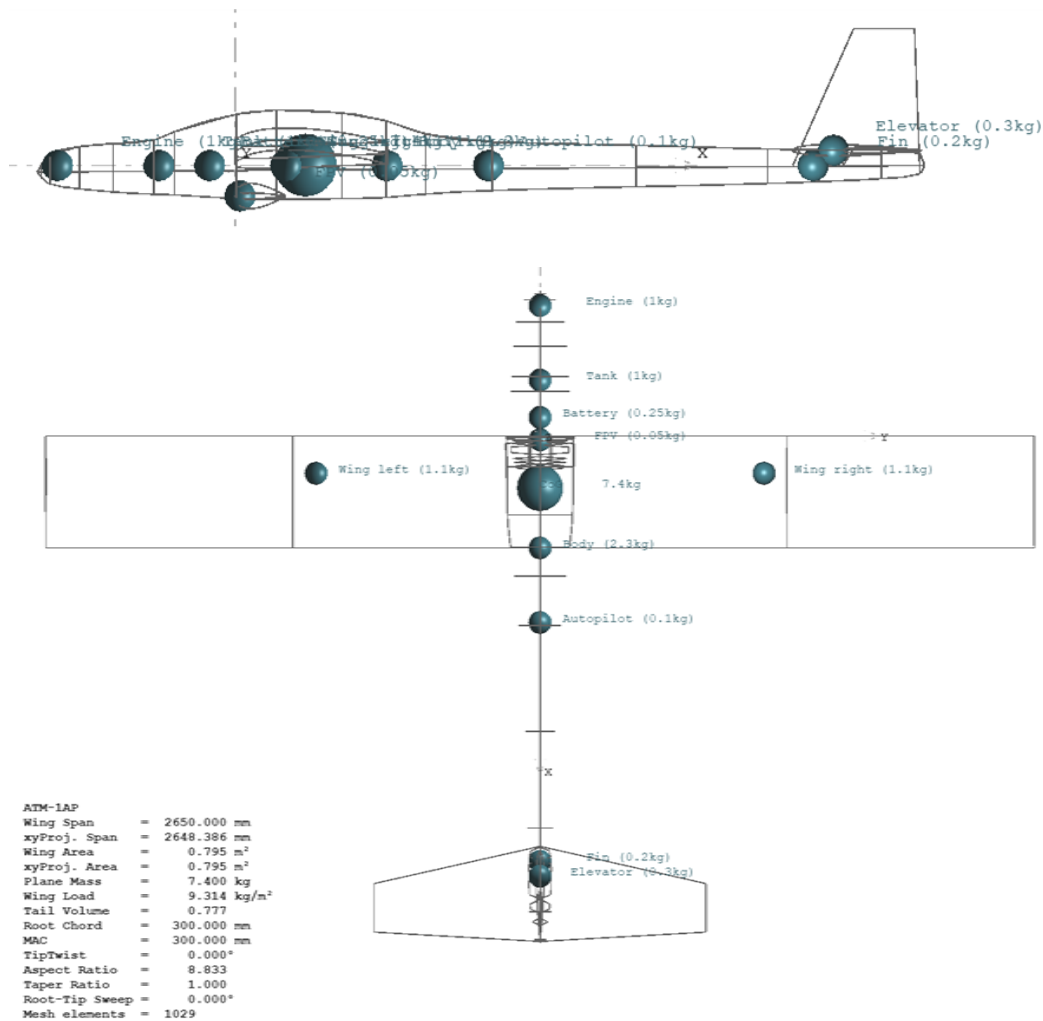


FIG. 11 ATM-1AP balancing

CONCLUSIONS

The implications of the ATM-1 UAV upgrade process require multiple iterations on aerodynamic and centerline optimization. The paper presented an aerodynamic optimization and centering cycle, which can form a foundation for completing the upgrade approach. Accurate digital reproduction of the geometry and layout of the inertial values can converge to results similar to those of the experimental stages. Mounting the FPV camera nacelle on the ventral side has minimal implications on aerodynamic performance, however an optimization of stability through the layout of the equipment is considered.

The optimal arrangement of the equipment determines the maximization of the UAV flight performances, correlated with the balancing limits determined by the fuel consumption or the release of some mass elements necessary for the missions in the areas of interest.

REFERENCES

- [1] *Unmanned Aircraft Systems*, available at <https://www.globalsecurity.org/military/world/uav.htm> accessed at 05.04.2023;
- [2] *Cartea tehnică a avionului Aero T.M.-1*, 1981, Tg Mureș, 27p;
- [3] *Pixhawk PX4 autopilot*, available at <https://ardupilot.org/plane/docs/common-pixhawk-overview.html#common-pixhawk-overview> , consulted at 12.05.2023;
- [4] *uRAD monitor A3*, available at <https://www.uradmonitor.com/products> , consulted at 12.05.2023;
- [5] *FR Sky Taranis*, available at <https://www.frsky-rc.com/product/taranis-x9d-plus-2> consulted at 14.05.2023;
- [6] *Guidelines for XFLR5 v6.03. Analysis of foils and wings operating at low Reynolds numbers*, 71 p. 2013, available at <https://sourceforge.net/projects/xflr5/>;
- [7] Ardupilot, available at <https://ardupilot.org/copter/docs/common-powering-the-pixhawk.html> , consulted at 14.05.2023;
- [8] V. Prisacariu, M. Boșcoianu, I. Cîrciu, *Management of robotic aerial systems accomplishment*, RECENT Journal 2/2012, Transilvania University of Brasov, Romania, ISSN 1582-0246, p. 203-217;
- [9] *Gasoline engine*, available at <https://www.zyhobby.com/products/rcgf-26cc-petrol-gasoline-engine>, consulted at 14.05.2023;
- [10] *Clark Y airfoil*, <http://airfoiltools.com/airfoil/details?airfoil=clarkysm-il>, accessed at 11.05.2023;
- [11] Shakhathreh, Hazim, Sawalmeh, Ahmad, Al-Fuqaha, Ala, Dou, Zuochoao & Almaitta, Eyad, Khalil, Issa, Othman, Noor, Khreishah, Abdallah, Guizani, Mohsen. (2019). *Unmanned Aerial Vehicles (UAVs): A Survey on Civil Applications and Key Research Challenges*. IEEE Access. 7., <https://doi.org/10.1590/jatm.v13.1233>;
- [12] J.P. Yaacoub, H. Noura, O. Salman, A. Chehab, *Security analysis of drones systems: Attacks, limitations, and recommendations*, Internet of Things, Volume 11, 2020, 100218, ISSN 2542-6605, <https://doi.org/10.1016/j.iot.2020.100218>.

Annex 1. 2D analysis. Aerodynamic coefficients.

Calculated polar for: NACA 0009											Calculated polar for: CLARK Y AIRFOIL										
1 Reynolds number fixed						Mach number fixed					1 Reynolds number fixed						Mach number fixed				
alpha	Cl	CD	Cl/D	Cm	Cm0	Cl	CD	Cl/D	Cm	Cm0	alpha	Cl	CD	Cl/D	Cm	Cm0	Cl/D	Cm	Cm0		
-15.000	-0.7397	0.12038	6.1439	0.17099	0.0000	0.0000	0.0000	0.0000	0.0000	0.0000	-12.000	-0.6087	0.12487	4.8746	-0.0311	1.0000	0.0006	-2.3950	0.0000	0.0000	
-12.000	-0.7183	0.11975	6.0836	0.2006	0.0000	0.0000	0.0000	0.0000	0.0000	0.0000	11.000	0.1755	0.11708	0.15124	0.0342	1.0000	0.0101	2.0042	0.0000	0.0000	
-9.000	-0.7012	0.11954	6.0496	0.2027	1.0000	0.0000	0.0000	0.0000	0.0000	0.0000	9.000	0.1264	0.02184	0.02485	-0.0919	0.9612	0.0416	1.6273	0.0000	0.0000	
-6.000	-0.6875	0.11952	6.0424	0.2027	1.0000	0.0000	0.0000	0.0000	0.0000	0.0000	6.000	-0.1824	0.03475	0.04175	-0.0658	0.9411	0.0441	1.2413	0.0000	0.0000	
-3.000	-0.6776	0.11958	6.0454	0.2027	1.0000	0.0000	0.0000	0.0000	0.0000	0.0000	3.000	0.0722	0.05178	0.06241	0.0078	0.8413	0.0958	1.5424	0.0000	0.0000	
0.000	0.0000	0.0000	0.0000	0.0000	1.0000	0.0000	0.0000	0.0000	0.0000	0.0000	0.000	0.1917	0.00078	0.00029	-0.0041	0.2051	0.1000	1.1741	0.0000	0.0000	
3.000	0.6776	0.11958	6.0454	0.2027	1.0000	0.0000	0.0000	0.0000	0.0000	0.0000	3.000	0.0722	0.05178	0.06241	0.0078	0.8413	0.0958	1.5424	0.0000	0.0000	
6.000	0.6875	0.11952	6.0424	0.2027	1.0000	0.0000	0.0000	0.0000	0.0000	0.0000	6.000	0.1264	0.02184	0.02485	-0.0919	0.9612	0.0416	1.6273	0.0000	0.0000	
9.000	0.7012	0.11954	6.0496	0.2027	1.0000	0.0000	0.0000	0.0000	0.0000	0.0000	9.000	0.1755	0.11708	0.15124	0.0342	1.0000	0.0101	2.0042	0.0000	0.0000	
12.000	0.7183	0.11975	6.0836	0.2006	0.0000	0.0000	0.0000	0.0000	0.0000	0.0000	12.000	0.7397	0.12038	6.1439	0.17099	0.0000	0.0000	0.0000	0.0000	0.0000	
15.000	0.7397	0.12038	6.1439	0.17099	0.0000	0.0000	0.0000	0.0000	0.0000	0.0000	15.000	0.7728	0.12085	6.1905	0.16051	0.0000	0.0000	0.0000	0.0000	0.0000	

Annex 2. 3D analysis. Aerodynamic coefficients.

NACA 0009											CLARK Y AIRFOIL										
1 Reynolds number fixed						Mach number fixed					1 Reynolds number fixed						Mach number fixed				
alpha	Cl	CD	Cl/D	Cm	Cm0	alpha	Cl	CD	Cl/D	Cm	Cm0	alpha	Cl	CD	Cl/D	Cm	Cm0	alpha	Cl	CD	
-15.000	-0.6875	0.11952	6.0424	0.2027	1.0000	-15.000	-0.6875	0.11952	6.0424	0.2027	1.0000	-15.000	-0.6875	0.11952	6.0424	0.2027	1.0000	-15.000	-0.6875	0.11952	
-12.000	-0.6875	0.11952	6.0424	0.2027	1.0000	-12.000	-0.6875	0.11952	6.0424	0.2027	1.0000	-12.000	-0.6875	0.11952	6.0424	0.2027	1.0000	-12.000	-0.6875	0.11952	
-9.000	-0.6875	0.11952	6.0424	0.2027	1.0000	-9.000	-0.6875	0.11952	6.0424	0.2027	1.0000	-9.000	-0.6875	0.11952	6.0424	0.2027	1.0000	-9.000	-0.6875	0.11952	
-6.000	-0.6875	0.11952	6.0424	0.2027	1.0000	-6.000	-0.6875	0.11952	6.0424	0.2027	1.0000	-6.000	-0.6875	0.11952	6.0424	0.2027	1.0000	-6.000	-0.6875	0.11952	
-3.000	-0.6875	0.11952	6.0424	0.2027	1.0000	-3.000	-0.6875	0.11952	6.0424	0.2027	1.0000	-3.000	-0.6875	0.11952	6.0424	0.2027	1.0000	-3.000	-0.6875	0.11952	
0.000	0.0000	0.0000	0.0000	0.0000	1.0000	0.000	0.0000	0.0000	0.0000	0.0000	1.0000	0.000	0.0000	0.0000	0.0000	0.0000	1.0000	0.000	0.0000	0.0000	
3.000	0.6875	0.11952	6.0424	0.2027	1.0000	3.000	0.6875	0.11952	6.0424	0.2027	1.0000	3.000	0.6875	0.11952	6.0424	0.2027	1.0000	3.000	0.6875	0.11952	
6.000	0.6875	0.11952	6.0424	0.2027	1.0000	6.000	0.6875	0.11952	6.0424	0.2027	1.0000	6.000	0.6875	0.11952	6.0424	0.2027	1.0000	6.000	0.6875	0.11952	
9.000	0.6875	0.11952	6.0424	0.2027	1.0000	9.000	0.6875	0.11952	6.0424	0.2027	1.0000	9.000	0.6875	0.11952	6.0424	0.2027	1.0000	9.000	0.6875	0.11952	
12.000	0.6875	0.11952	6.0424	0.2027	1.0000	12.000	0.6875	0.11952	6.0424	0.2027	1.0000	12.000	0.6875	0.11952	6.0424	0.2027	1.0000	12.000	0.6875	0.11952	
15.000	0.6875	0.11952	6.0424	0.2027	1.0000	15.000	0.6875	0.11952	6.0424	0.2027	1.0000	15.000	0.6875	0.11952	6.0424	0.2027	1.0000	15.000	0.6875	0.11952	

Annex 3. Balance export data.

```

# Mass & Inertia breakdown.
# x y z is location of item's own CG.
# Ixx... are item's inertias about item's own CG.
#
# x,y,z system here must be exactly the same one used in the .avl input file
# (same orientation, same origin location, same length units)
#
# mass      X      Y      Z      Ixx      Iyy      Izz      Ixy      Ixz      Iyz
0      0      126      1.75e+14      31.1      0      0      0      0      0
0      0      42.2      -4.04e+15      -60      0      0      0      0      0
0      0.123e+03      7.7e+14      -30      0      0      0      0      0
0      0.123e+03      -1.60e+13      1025      0      0      0      0      0
1      -350      0      0      0.000      0.000      0.000      0.000      0.000      0.000
1      -150      0      0      0.000      0.000      0.000      0.000      0.000      0.000
0.25      -50      0      0      0.000      0.000      0.000      0.000      0.000      0.000
1.1      100      600      0      0.000      0.000      0.000      0.000      0.000      0.000
1.1      100      -600      0      0.000      0.000      0.000      0.000      0.000      0.000
0.05      10      0      -60      0.000      0.000      0.000      0.000      0.000      0.000
0.3      1.18e+03      0      30      0.000      0.000      0.000      0.000      0.000      0.000
0.2      1.18e+03      0      0      0.000      0.000      0.000      0.000      0.000      0.000
2.3      300      0      0      0.000      0.000      0.000      0.000      0.000      0.000
0.1      500      0      0      0.000      0.000      0.000      0.000      0.000      0.000
    
```